Supplementary Material for

Construction of bifunctional electrochemical biosensors for the sensitive detection of SARS-CoV-2

N-gene based on porphyrin porous organic polymers

Jing Cui, Lun Kan, Fang Cheng, Jiameng Liu, Linghao He, Yulin Xue, Shaoming Fang*, Zhihong Zhang*

College of Material and Chemical Engineering, Zhengzhou University of Light Industry, No. 136, Science Avenue, Zhengzhou 450001, P. R. China

* Corresponding authors

E-mail addresses: mingfang@zzuli.edu. cn, mainzhh@163.com (Z. Zhang)

Content

S1. Experimental section

S1.1 Materials and Chemicals

2,2'-bipyridyl-5,5'-dialdehyde (DPDD), 5,10,15,20-tetra (4-aminophenyl) porphyrin (TAPP) were purchased from Kaishu Chemical Technology Co., Ltd. (Shanghai, China). o-dichlorobenzene, n-butyl alcohol were obtained from Shanghai Aladdin Biochemical Technology Co., Ltd (Shanghai, China). Acetone, hydrogen peroxide and disodium hydrogen phosphate were purchased from Luoyang Haohua Chemical Reagent Co., Ltd (Henan, China). 1, 4-dioxane and glacial acetic acid were supplied by Tianjin Fuyu Fine Chemicals Co., Ltd (Tianjin, China). All of the other chemicals are analytical reagent grade and used without further purification. Milli-Q water (18.2 Ω cm resistivity at 25 °C) was used throughout the experiments.

Potassium ferrocyanide trihydrate and potassium ferricyanide were supported by Sinopharm chemical reagent Co., Ltd. (Shanghai, China). Bovine serum albumin (BSA) and immune globulin (IgG) were purchased from Beijing Solarbio Science & technology Co., Ltd. (Beijing, China). Influenza A Virus (FluA), Influenza B Virus (FluB), Myocoplasima pneumonia (P1) and Chlamydia pneumoniae (CPN) were obtained from Oneclone Biotechnology Co., Ltd. (Xiamen, China). N-gene aptamer N58 were supplied by Sangon Biotech Co., Ltd. (Shanghai, China). SARS-CoV-2 N-gene was obtained from CUSABIO BIOTECH CO.,Ltd. (Wuhan, China). SARS-CoV-2 N-gene Antibody Protein was purchased from Beijing Biodragon Immunotechnologies Co., Ltd. (Beijing, China). The sequence of the N58 aptamer was as follows: GCT GGA TGT CAC CGG ATT GTC GGA CAT CGG ATT GTC TGA GTC ATA TGA CAC ATC CAG C.

S1.2 Preparation of All Solutions

Herein, phosphate buffer solution (PBS, 0.1 M, pH = 7.4) was used as the biological buffer, which was prepared by mixing 0.242 g KH_2PO_4, 1.445 g $Na_2HPO_4 \cdot 12H_2O$, 0.2 g KCl, and 8.003 g NaCl in Milli-Q water. The solution was then adjusted to pH 7.4 by adding 0.1 M HCl solution. The electrolyte solution was prepared immediately before use by dissolving 1.65 g $K_3Fe(CN)_6$, 2.11 g $K_4Fe(CN)_6 \cdot 3H_2O$ and 7.5 g KCl in PBS (1.0 L).

The stock solution of aptamer (100 nM), both N-gene aptamer solutions and antibody solutions of different concentrations (0, 0.0001, 0.001, 0.01, 0.1, 1, 10, 100 and 1000 pg mL^{-1}) and other solution were prepared using 0.01 M PBS (pH 7.4) and stored at 4 °C.

S1.3 Pretreatment of Bare Au Electrode (AE)

A bare AE with diameter of 3.0 mm obtained from Gaoss Union instrument Inc. (http://www.gaossunion.cn) was employed as working electrode. Before used, the bear AE was cleaned by following steps: Firstly, the AE was polished with 0.3 and 0.05 μm alumina powder to obtain a mirror-like surface, and rinsed with ultrapure water for 2 min. Afterward, the AE was washed with piranha solution (v/v, H_2SO_4/H_2O_2 = 7/3) and ethanol for 15 min, respectively. Afterward, the AE was washed with Milli-Q water and dried under nitrogen. The AE was electrochemically activated in 0.5 M H_2SO_4 within the potential cycling between −0.2 V and 1.6 V. Finally, the AE was rinsed with Milli-Q water and dried under nitrogen again, and stored for further use.

S1.4 Basic Characterizations

The chemical components were characterized by Fourier Transform Infrared Spectroscopy (FT-IR) using a Bruker TENSOR27 spectrometer (Germany) (32 scans at 4 cm^{-1} resolution). X-ray photoelectron spectroscopy (XPS) was employed to determine using an AXIS HIS 165 spectrometer (Kratos Analytical, Manchester, U.K.)

with a monochromatized Al K_α X-ray source (1486.71 e K_αV photons). The structure of the synthesized TAPP-DPDD-POP were investigated by X-ray diffraction with Cu K_α radiation (λ = 0.15406 nm) (XRD, D/MAX-2500V/PC, Rigaku, Japan). The surface morphology of the synthesized samples was performed with JSM-6490LV field emission scanning electron microscope (FE-SEM) and JEOL JEM-2100 high-resolution transmission electron microscopy (HR-TEM) with a field emission gun of 200 kV. N_2 adsorption and desorption data were taken on a Belsorp MAX volumetric sorption equipment with a diaphragm and turbo pumping system under ultra-high vacuum. The elemental mapping were measured by energy dispersive spectrometer (EDS, XFlash-5030T, Bruker) on TEM.

S1.5 Electrochemical Measurements

Electrochemical measurements, including electrochemical impedance spectroscopy (EIS) and cyclic voltammetry (CV), were carried out using CHI 760E (CH Instruments Inc., Shanghai) electrochemical workstation equipped with a conventional three-electrode cell with 5 mM $K_3[Fe(CN)_6]$/$K_4[Fe(CN)_6]$ (1:1) as the electrolyte solution, a platinum wire as the counter electrode, a silver/silver chloride (Ag/AgCl) electrode as the reference electrode and AE or modified AE as the working electrode. The cyclic voltammetry (CV) was performed from −0.2 V to 0.8 V at the scan rate of 100 mV s^{-1}. Electrochemical impedance spectra (EIS) curves were recorded within the frequency range of 0.01 Hz–100 kHz with an amplitude of 5 mV (EIS parameters: potential, 0.21 V; frequency range, 100 kHz−0.01 Hz; room temperature), as shown in **Fig. S1**. The incubation and testing temperatures are room-temperature. The EIS spectra were analyzed using Zview2 software from Scribner Associates Incorporated, which utilizes nonlinear least-squares fitting to determine element parameters in the equivalent circuit (**Fig. S1 inset**). The equivalent circuit is composed of solution resistance (R_s), charge-transfer resistance (R_{ct}), constant-phase element (CPE), and Warburg impedance (W_o). Each test was repeated at least three times.
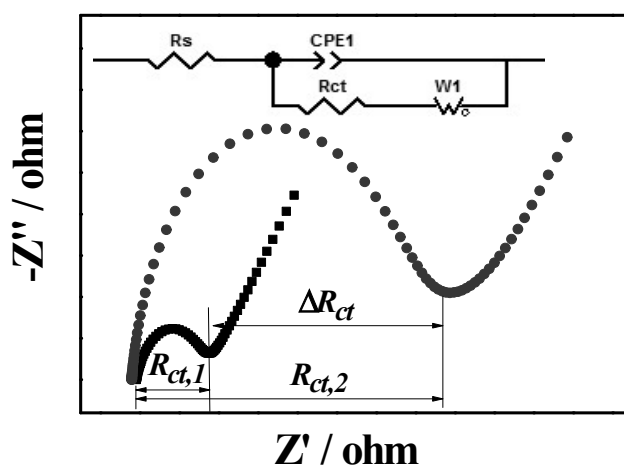
Fig. S1. Typical EIS Nyquist plots and equivalent circuit.

S1.6 Pretreated of real samples

Human serum was obtained from Beijing Solarbio Science & Technology Co., Ltd. In prior to use, it was filtered using a 3 kDa dialysis bag to remove possible interfered compounds, then it was left at room temperature for 0.5 h and centrifuged at 2000 r min^{-1} for 10 min. The resultant supernatant serum was separated and stored at - 20 °C.

Since it is difficult to contact the SARS-CoV-2 patients, saliva were collected though normal patients. After diluted for 1000 times by PBS, the saliva were filtered through a mixed cellulose ester membrane (0.22 μm). The seawater were obtained from the Taiwan Strait in the East China Sea near Xiamen, and was filtered through a mixed cellulose ester membrane (0.22 μm). The frozen seafood was purchased from the Dazhang supermarket of Zhengzhou, China, triturated and further transferred to a 150 mL centrifuge tube. Afterward, the sample was centrifuged at 1000 rpm for 5 min at room temperature. At last, the supernatant was collected for further use.

S2. **Basic characterizations of TAPP-DPDD-POP**
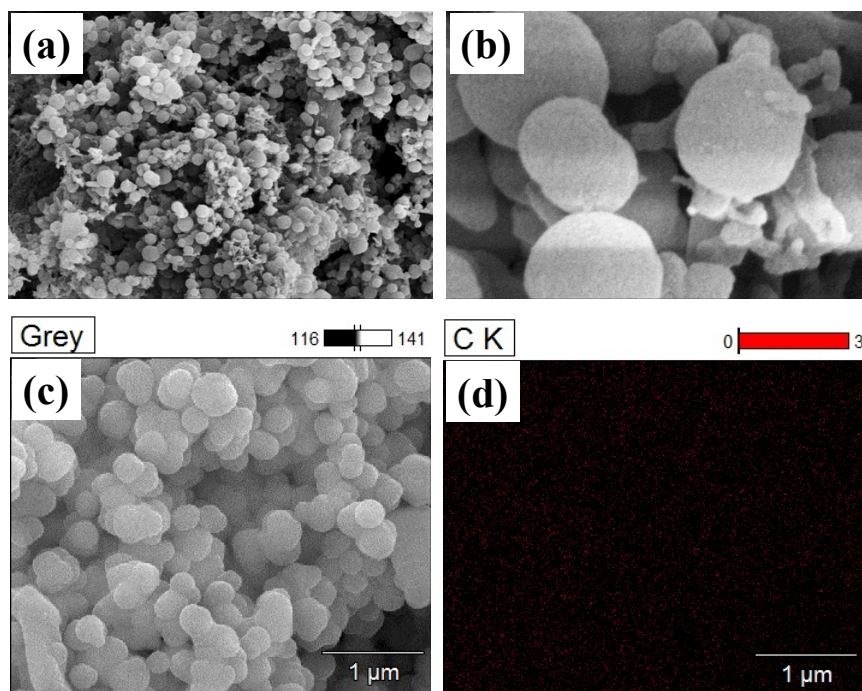
Fig. S2 Basic characterization, including (a) Low- and (b) high-magnification SEM images and (c, d) EDS spectra of TAPP-DPDD-POP.
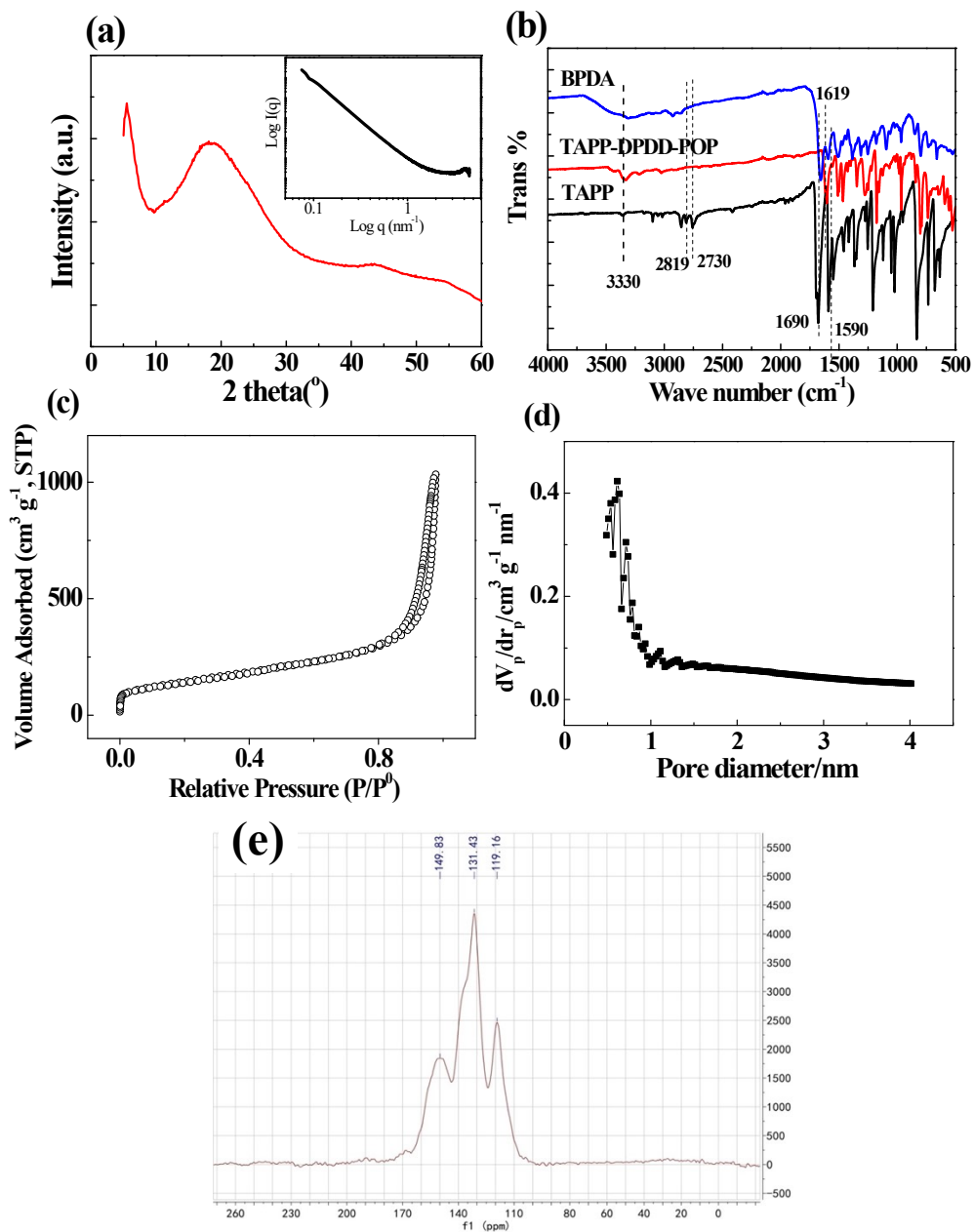
Fig. S3 Basic characterization, including (a) WAXS (Insert SAXS), (b) FT-IR, (c) N_2 sorption isotherm, (d) pore diameter distribution and (e) ^{13}C NMR of TAPP-DPDD-POP.

S3. Optimization of the detection parameters of TAPP-DPDD-POP-based aptasensor
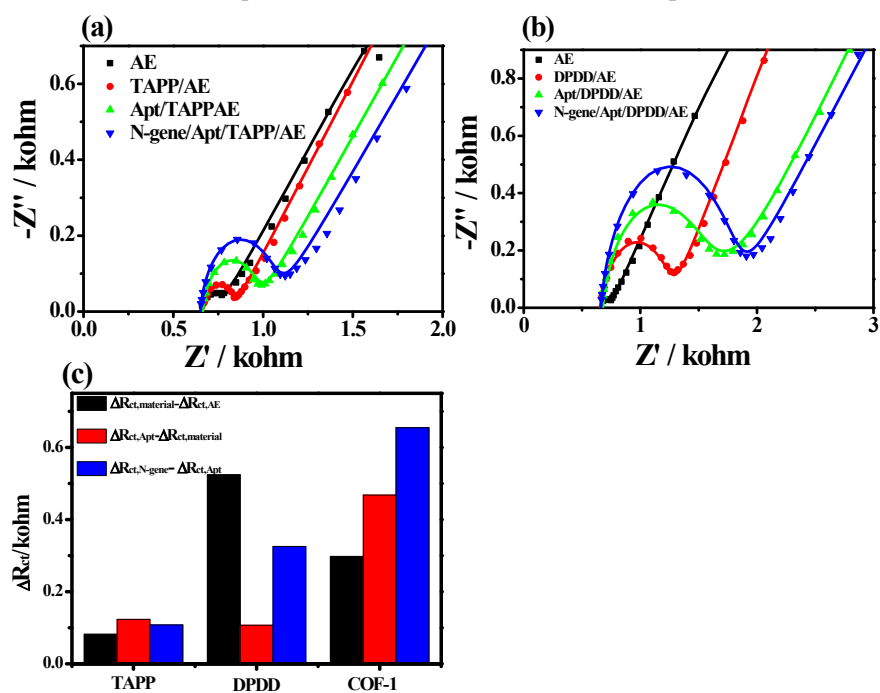
Fig. S4 EIS responses of (a) TAPP-based and (b) DPDD-based aptasensor fabricating process and N-gene detection; (c) The ΔR_{ct} values of the aptasensors based on TAPP, DPDD, and TAPP-DPDD-POP for detecting N-gene.
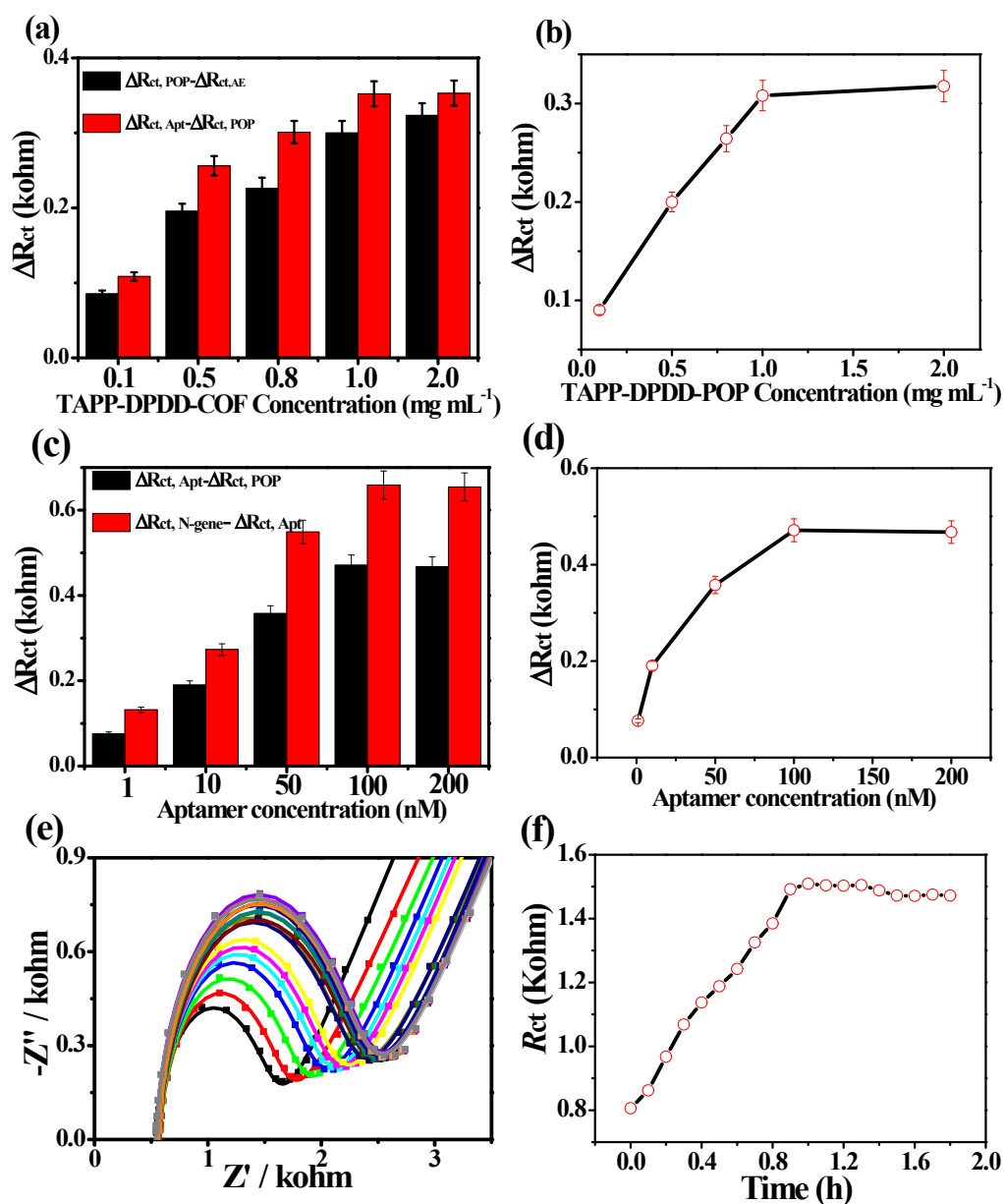
Fig. S5 Variation in charge-transfer resistance (ΔR_{ct}) for the detection of SARS-CoV-2 N-gene by (a, b) using the TAPP-DPDD-POP-based aptasensors developed with TAPP-DPDD-POP with concentration of 0.1, 0.5, 0.8, 1.0, 2.0 mg mL^{-1}. (c, d) The caused ΔR_{ct} values by the N-gene aptamer solutions with different concentrations (1, 10, 50, 100 and 200 nM). (e, f) The R_{ct} values as function of binding time of the N-gene aptamer and SARS-CoV-2 N-gene.

S4 Optimization of the detection paramet of TAPP-DPDD-POP-based immunosensor
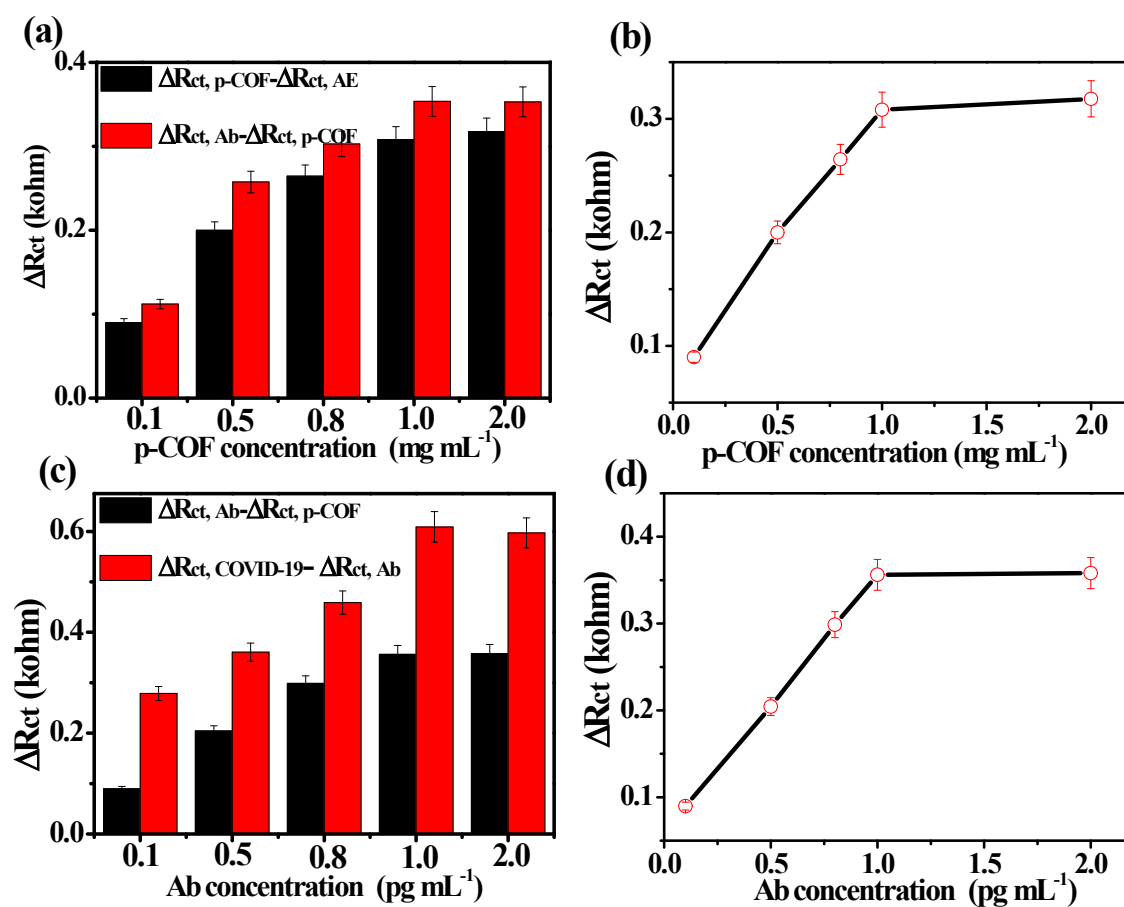
Fig. S6 (a,b) The change of ΔR_{ct} of using the TAPP-DPDD-POP-based immunosensors developed with TAPP-DPDD-POP with concentration of 0.1, 0.5, 0.8, 1.0, 2.0 mg mL^{-1}. (c, d) The caused ΔR_{ct} values by the N-gene antibody solutions with different concentrations (0.1, 0.5, 0.8, 1.0 and 2.0 pg mL^{-1}) for the detection of SARS-CoV-2 N-gene using the TAPP-DPDD-POP-based aptasensor.

S5. Detection of SARS-CoV-2 N-gene by TAPP-DPDD-POP-based aptasensor and immunosensor

Table S1 Comparison with other reported techniques for SARS-CoV-2 N-gene detection based on aptasensor method.

Materials	Detection method	Detection range	LOD	Refs.
–	Aptamer-assisted proximity ligation assay	50–5000 pg mL^{-1}	37.5 pg mL^{-1}	1
DNA tetrahedron	Electrochemiluminescence (ECL)	1 fM–100 pM	2.67 fM	2
–	Reverse transcription-LAMP	–	1.02 fg mL^{-1}	3
Calixarene functionalized graphene oxide	Electrochemical	–	200 copies mL^{-1}	4
Gold nano-film	Surface plasmon resonance (SPR)	25–1000 nM	37 nM	5
–	Surface-enhanced Raman scattering (SERS)	0–1000 PFU/mL	10PFU/mL	6
Graphene oxide	(GO) coated optical microfiber SPR and EMSA	10^{-18}–10^{-7} M	1 × 10^{-9} M	7
TAPP-DPDD-POP	**electrochemical**	**1 fg mL^{-1}–1 ng mL^{-1}**	**0.17 fg mL^{-1}**	**This work**

Table S2 Comparison with other reported techniques for SARS-CoV-2 N-gene detection based on immunosensor method.

Materials	Detection method	Detection range	LOD	Refs.
Co-Fe@hemin-peroxidase	Nanozyme-based chemiluminescence paper	0.2–100 ng mL^{-1}	0.1 ng mL^{-1}	8
Carbon black nanomaterial	Electrochemical	0.1–16 nM	8 ng mL^{-1}	9
Single-walled carbon nanotube	Field-effect transistor	–	0.55 fg mL^{-1}	10
Laminated films	ELISA	1–50 ng μL^{-1}	9.00 ng μL^{-1}	11
Carboxylic red latex beads	Lateral flow assays (LFAs)	0.53–0.77 ng mL^{-1}	0.65 ng mL^{-1}	12
Reduced Graphene Oxide (rGO)	Electrochemical	0.16–40 μg mL^{-1}	150 ng mL^{-1}	13
TAPP-DPDD-POP	**Electrochemical**	**1 fg mL^{-1} to 1 ng mL^{-1}**	**0.17 fg mL^{-1}**	**This work**

S6. Detection of SARS-CoV-2 N-gene in real samples by TAPP-DPDD-POP- based aptasensor and immunosensor

Table S3 Detection of SARS-CoV-2 N-gene in human serum by TAPP-DPDD-POP-based aptasensor.

Amount added (pg mL^{-1})	Found amount (pg mL^{-1})	Apparent recovery (%)	RSD (%)
0.001	0.000972	97.2	2.663
0.01	0.010143	101.4	2.392
0.1	0.100570	100.5	3.349
1	1.089023	108.9	0.695
10	9.719733	97.1	4.548
100	104.3562	104.3	1.208
1000	1028.834	102.8	3.389

Table S4 Detection of SARS-CoV-2 N-gene in throat swab by TAPP-DPDD-POP-based aptasensor.

Amount added (pg mL^{-1})	Found amount (pg mL^{-1})	Apparent recovery (%)	RSD (%)
0.001	0.001089	108.9	1.277
0.01	0.010585	105.8	4.159
0.1	0.107365	107.3	1.044
1	0.966463	96.6	3.411
10	10.936765	109.3	1.620
100	110.461	110.4	2.351
1000	992.918	99.2	3.682

Table S5 Detection of SARS-CoV-2 N-gene in seawater by TAPP-DPDD-POP-based aptasensor.

Amount added (pg mL^{-1})	Found amount (pg mL^{-1})	Apparent recovery (%)	RSD (%)
0.001	0.0009845	98.4	1.617
0.01	0.0105700	105.7	2.463
0.1	0.1072129	107.2	4.199
1	0.9719733	97.1	1.295
10	11.6757275	116.7	4.442
100	108.747618	108.7	3.854
1000	1103.04338	110.3	3.101

Table S6 Detection of SARS-CoV-2 N-gene in frozen seafood by TAPP-DPDD-POP-based aptasensor.

Amount added (pg mL^{-1})	Found amount (pg mL^{-1})	Apparent recovery (%)	RSD (%)
0.001	0.000987	98.7	0.936
0.01	0.010071	100.7	3.083
0.1	0.112842	112.8	4.179
1	0.951470	95.1	2.537
10	10.813110	108.1	1.931
100	105.100538	105.1	1.584
1000	965.09019	96.5	3.259

Table S7 Detection of SARS-CoV-2 N-gene in human serum by TAPP-DPDD-POP-based immunosensor.

Amount added (pg mL^{-1})	Found amount (pg mL^{-1})	Apparent recovery (%)	RSD (%)
0.001	0.000963	96.3	2.987
0.01	0.009924	99.2	0.869
0.1	0.102908	102.9	1.537
1	1.059001	105.9	3.048
10	9.625039	96.2	1.237
100	107.9431	107.9	2.506
1000	1034.993	103.4	3.472

Table S8 Detection of SARS-CoV-2 N-gene in throat swab by TAPP-DPDD-POP-based immunosensor.

Amount added (pg mL^{-1})	Found amount (pg mL^{-1})	Apparent recovery (%)	RSD (%)
0.001	0.000944	94.4	1.212
0.01	0.009717	97.17	2.073
0.1	0.106917	106.9	2.939
1	0.981073	98.1	1.753
10	11.002561	110.0	2.904
100	104.393197	104.3	0.928
1000	1089.793964	108.9	3.057

Table S9 Detection of SARS-CoV-2 N-gene in seawater by TAPP-DPDD-POP-based immunosensor.

Amount added (pg mL^{-1})	Found amount (pg mL^{-1})	Apparent recovery (%)	RSD (%)
0.001	0.0009886	98.8	1.101
0.01	0.0102417	102..4	2.594
0.1	0.1053954	105.3	3.592
1	0.9717440	97.1	3.653
10	9.8577076	98.5	0.979
100	110.869804	110.8	1.717
1000	1004.78857	100.4	2.013

Table S10 Detection of SARS-CoV-2 N-gene in frozen seafood by TAPP-DPDD- POP-based immunosensor.

Amount added (pg mL^{-1})	Found amount (pg mL^{-1})	Apparent recovery (%)	RSD (%)
0.001	0.000988	98.8	2.559
0.01	0.009625	96.2	2.128
0.1	0.101637	101.6	0.905
1	1.076342	107.6	1.628
10	10.971069	109.7	3.121
100	104.592869	104.5	1.594
1000	1035.98316	103.5	0.991

References

1. R. Liu, L. He, Y. Hu, Z. Luo and J. Zhang, *Chemical Science*, 2020, **11**, 12157-12164.

2. Z. Fan, B. Yao, Y. Ding, J. Zhao, M. Xie and K. Zhang, *Biosensors and Bioelectronics*, 2021, **178**, 113015.

3. L. E. Lamb, S. N. Bartolone, E. Ward and M. B. Chancellor, *medRxiv*, 2020, DOI: 10.1101/2020.02.19.20025155, 2020.2002.2019.20025155.

4. H. Zhao, F. Liu, W. Xie, T.-C. Zhou, J. OuYang, L. Jin, H. Li, C.-Y. Zhao, L. Zhang, J. Wei, Y.-P. Zhang and C.-P. Li, *Sensors and Actuators B-Chemical*, 2021, **327**, 128899.

5. J. Li and P. B. Lillehoj, *ACS Sensors*, 2021, **6**, 1270-1278.

6. H. Chen, S.-G. Park, N. Choi, H.-J. Kwon, T. Kang, M.-K. Lee and J. Choo, *ACS Sensors*, 2021, **6**, 2378-2385.

7. H. Jia, A. Zhang, Y. Yang, Y. Cui, J. Xu, H. Jiang, S. Tao, D. Zhang, H. Zeng, Z. Hou and J. Feng, *Lab on a Chip*, 2021, **21**, 2398-2406.

8. D. Liu, C. Ju, C. Han, R. Shi, X. Chen, D. Duan, J. Yan and X. Yan, *Biosensors and Bioelectronics*, 2021, **173**, 112817.

9. L. Fabiani, M. Saroglia, G. Galatà, R. De Santis, S. Fillo, V. Luca, G. Faggioni, N. D'Amore, E. Regalbuto, P. Salvatori, G. Terova, D. Moscone, F. Lista and F. Arduini, *Biosensors & Bioelectronics*, 2021, **171**, 112686.

10. W. Shao, M. R. Shurin, S. E. Wheeler, X. He and A. Star, *ACS Applied Materials & Interfaces*, 2021, **13**, 10321-10327.

11. S. Kasetsirikul, M. Umer, N. Soda, K. R. Sreejith, M. J. A. Shiddiky and N.-T. Nguyen, *Analyst*, 2020, **145**, 7680-7686.

12. B. D. Grant, C. E. Anderson, J. R. Williford, L. F. Alonzo, V. A. Glukhova, D. S. Boyle, B. H. Weigl and K. P. Nichols, *Analytical Chemistry*, 2020, **92**, 11305-11309.

13. G. C. Zaccariotto, M. K. L. Silva, G. S. Rocha and I. Cesarino, *Materials*, 2021, **14**.